

## A Review of Molecular Dynamics Studies on Silica and Silicate Melts((A)Amorphous Alloys)

著者	Ogawa Hiroshi, Waseda Yoshio
journal or publication title	Science reports of the Research Institutes, Tohoku University. Ser. A, Physics, chemistry and metallurgy
volume	36
number	1
page range	20-35
year	1991-03-25
URL	<a href="http://hdl.handle.net/10097/28363">http://hdl.handle.net/10097/28363</a>

## A Review of Molecular Dynamics Studies on Silica and Silicate Melts\*

Hiroshi Ogawa<sup>†</sup> and Yoshio Waseda

Research Institute of Mineral Dressing and Metallurgy (SENKEN)

( Received January 17, 1991 )

### Synopsis

Current progress of molecular dynamics (MD) simulation on silicate melts has been summarized for recent 15 years. MD simulation is now recognized as one of the useful techniques for providing the short range ordering structures of the melt expressed by the radial distribution function. The long range ordering structures in the melt, on the other hand, have not fully investigated by MD simulation, and the number distribution of  $-(\text{Si-O})_n$  rings or chains is the unique index for characterizing the network structures of silicates. Transport properties and other atomistic dynamics for silicate melt have not also sufficiently investigated except for ionic diffusivity. For further development of the MD simulation studies, one of the most important subjects may be to prepare more physically reliable interatomic potentials which can be used for various composition of silicates.

### I. Introduction

Since the first molecular dynamics (MD) study of Woodcock *et al.*<sup>1</sup> on silica given in 1976, MD simulation has been widely used for analyzing the structures and properties of silica and silicates. Especially in the beginning of 1980's, many studies have been carried out on various compositions of silica and silicates in both molten and glassy states. The basic techniques of MD simulation seems to be completed in this period, and recent studies focus, more or less, on the specific subjects such as surface structures.

The purpose of MD simulation for silicate system may be summarized into the following three categories: investigation of crystal structures and rheological properties of silicates for geochemistry, characterization and design of silicates

---

\* The 91-R2 report of Institute for Research Institute of Mineral Dressing and Metallurgy (SENKEN)

† On leave from Kimura Metamelt Project, ERATO, Research Development Corporation of Japan (JRDC).

for glass science and metallurgical engineering, and an experimental tool for verifying a theoretical model for explaining the particular features of liquid and glassy silicates. Molecular dynamics simulation may be valuable in cases where conventional experiments are found to be technically difficult. High temperature, high pressure experiments, and time-consuming scan for many compositions might be the cases in point. Now MD simulation is recognized as a new 'experimental' technique, however, several important problems have been still unsolved in MD simulation for practical uses.

The purpose of this paper is to summarize the current progress in MD studies on silicates including its future prospects. The subjects matter is treated selectively rather than comprehensively and then the results of silicate melts are mainly included. Several important topics on glassy and crystalline states will also included for supplements.

## II. Interatomic Potentials

The interaction between silicon and oxygen may be characterized by the harmony of various factors such as ionicity, covalency, and directional dependence originated from  $sp^3$  orbital of silicon. Compared with other cation-oxygen pairs, the interaction of Si-O pairs has a large negative potential energy at the minimum. This strongly attractive potential contributes to the formation of the tight -Si-O- network structures in both molten and glassy states.

Various proposals are available for interatomic potentials for silica and silicates. They are classified into two types: pair potential and three-body potential. Both types may be further classified into empirical and non-empirical ones.

*Empirical pair potentials* : This type potential is given by an appropriate functional form and the relevant parameters determined so as to fit some macroscopic physical constants such as compressibility. For silicates, the Born-Mayer-Huggins type given by the following equation is widely used.

$$\phi_{ij}^{\text{BMH}}(r) = \frac{f^2 Z_i Z_j e^2}{4\pi\epsilon_0 r} + A_{ij} \exp\left(-\frac{\sigma_i + \sigma_j - r}{\rho_{ij}}\right) - \frac{C_i C_j}{r^6}, \quad (1)$$

where  $r$  is the distance between  $i$  and  $j$  species,  $Z$  is the formal charge of the ion,  $e$  is the electron charge (unit: C),  $\epsilon_0$  is the dielectric constant, and  $f$ ,  $A_{ij}$ ,  $\sigma_i$ ,  $\rho_{ij}$  and  $C_i$  are so-called potential parameters. Each terms in eq.(1) correspond to the Coulomb, repulsive, and dipole-dipole interactions, respectively. In the equation, for example, the number of potential parameters is sixteen in the case of  $M_2O-SiO_2$  system. (Note that the parameters  $A_{ij}$  and  $\sigma_i$  are not independent to each other.) Their determination is not an easy task. In

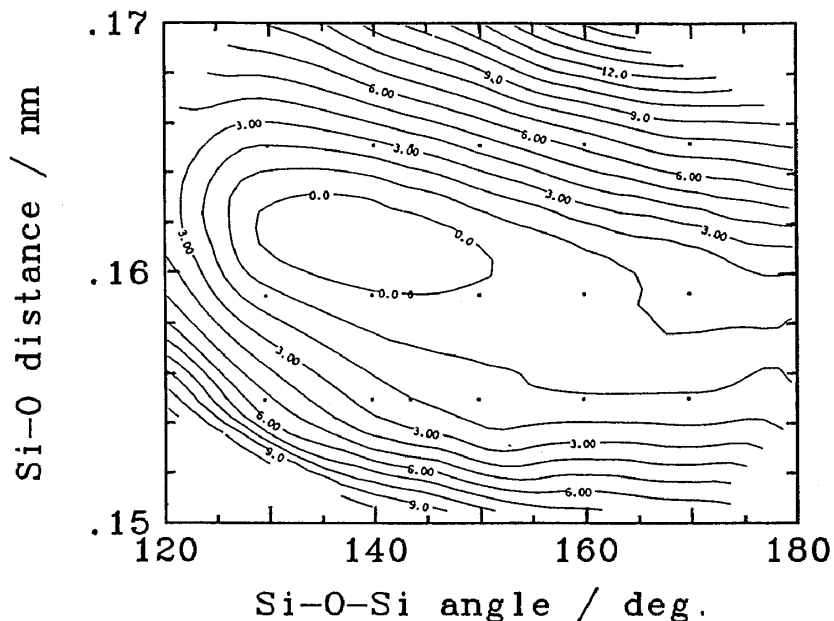


Fig. 1. The potential energy surface for  $H_6Si_2O_7$  cluster estimated by *ab initio* calculation (ref. 7). The numerical values in this figure are given in kcal/mol from the energy minimum.

order to reduce the number of independent parameters, the following approximations are usually employed:

$$f \simeq 1, \quad (2a)$$

$$\rho_{ij} \simeq \text{const.} = \rho, \quad (2b)$$

$$\rho_{ij} \simeq b_i + b_j, \quad (2c)$$

$$A_{ij} \simeq (b_i + b_j) \times 6.947 \times 10^{-11} N, \quad (2d)$$

$$c_i \simeq 0. \quad (2e)$$

Equation (1) with eqs.(2c) and (2d) is called Gilbert-Ida form.

Various experimental data are used for determining the potential parameters. They include the interference functions obtained by X-ray and neutron diffraction, stability of crystal structures, compressibility, etc. Even all of these data are taken into account, however, the potential parameters cannot be determined *a priori*. For this reason, several sets of the potential parameters are proposed, and their usefulness are discussed in the actual MD simulations.

Woodcock *et al.*<sup>1</sup> proposed numerical examples of potential parameters for silica. Mitra<sup>2</sup> used the potential form of Pauling type and proposed another set of parameters for silica. The potential parameters for alkali- and other silicates are proposed by Soules<sup>3</sup> and Kawamura.<sup>4</sup> For future convenience, the potential parameters proposed by them are listed in Table 1. It may be added that the empirical pair potentials for silicates are discussed in detail by Catlow *et al.*<sup>5</sup>

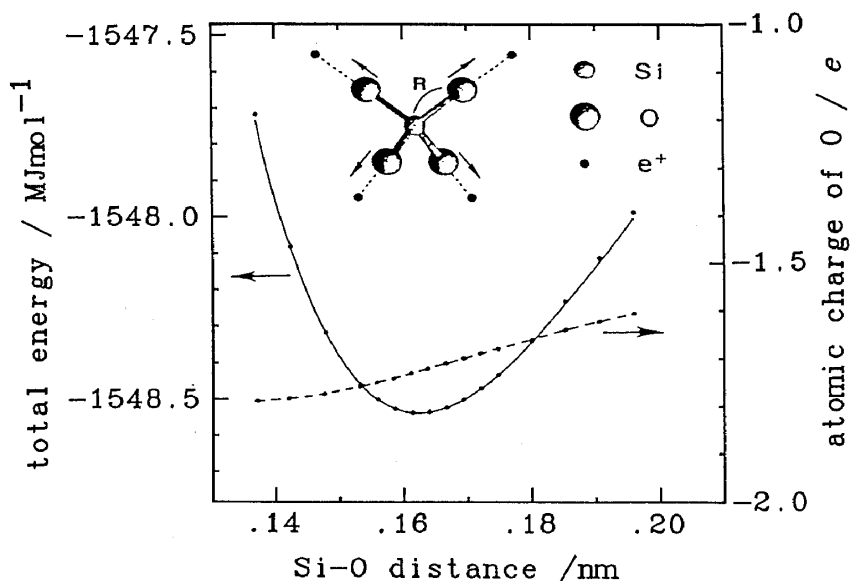


Fig. 2. Total energy and the atomic charge of oxygen estimated by *ab initio* calculation for  $\text{SiO}_4^{4-}-4e^+$  cluster (ref. 8).

*Non-empirical pair potentials* : The interatomic forces for Si-O and O-O pairs have been estimated from *ab initio* calculation on a small cluster of silica by Newton *et al.*<sup>6</sup> Recently two groups independently determined the non-empirical potentials for silica. Lasaga and Adams<sup>7</sup> (LA) calculated the potential surfaces concerning to the bending of  $\text{H}_6\text{Si}_2\text{O}_7$  cluster by Hartree-Fock self consistent field (HF-SCF) method as shown in Fig. 1. This approach enables us to reduce the potential parameters in the form of eq.(1) with full ionic charges. Using an  $\text{SiO}_4^{4-}-4e^+$  cluster, Tsuneyuki *et al.*<sup>8</sup> (TTAM) calculated the potential energy concerning to the deformation of tetrahedron (Fig. 2). They proposed the potential parameters with adopting the partial ionic charges of  $f = 0.6$ . The potential parameters proposed by these two groups are also listed in Table 1.

Procedures employed by these two groups are almost the same, but the final potential parameters proposed are considerably different. Such differences are illustrated in Fig. 3. The LA potentials are similar to those of Woodcock *et al.*<sup>1</sup> The TTAM potential, on the other hand, shows unrealistic behaviours in the region less than 0.15nm. This is mainly due to the dipole-dipole term. This unusual feature may not give a serious problem in simulation study at low temperature, but any correction should be required for high temperature study.

Any non-empirical potential for silicates has not been proposed yet.

*Three-body potentials* : Silicate structures characterized by 3-dimensional network are known to simulated by using pair potentials only. However, some reservations are automatically involved in the simulated structure because the information on directional dependence due to the covalent bond is not included in pair potentials. For this reason, it is desirable to include the three-body term

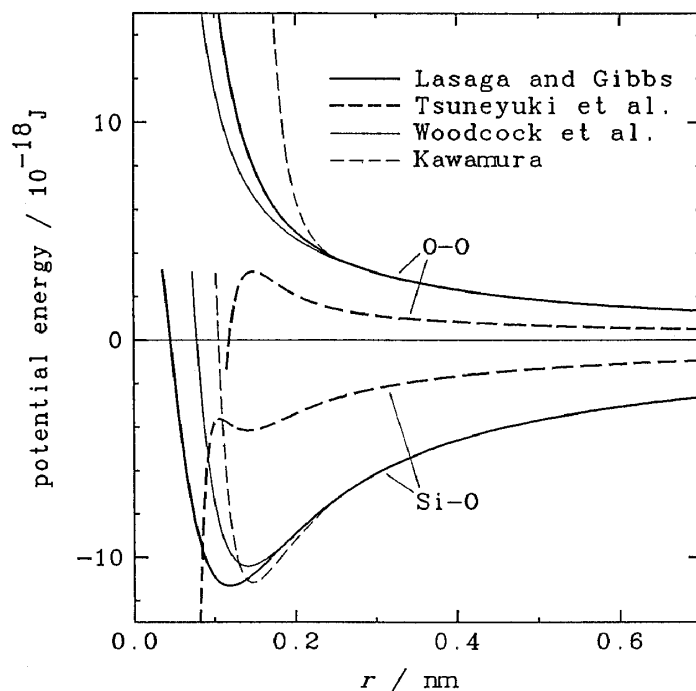


Fig. 3. Potentials for Si-O and O-O pairs proposed by several authors (refs. 1, 4, 7 and 8).

Table 1 Born-Mayer-Huggins Parameters for Silica and Silicates Proposed by Several Authors

authors	$f$	$i-j$	$A_{ij}/10^{-21}\text{J}$	$\sigma_{ij}/\text{nm}$	$\rho_{ij}/\text{nm}$	$C_{ij}/10^{-21}\text{J}\cdot\text{nm}^6$
Woodcock <sup>1</sup>	1.	O-O	4.05	.284	.029	0.
		Si-O	26.38	.275	.029	0.
		Si-Si	68.40	.266	.029	0.
Tsuneyuki <sup>3</sup>	0.6	O-O	2.441	.40948	.035132	0.03440
		Si-O	1.449	.29162	.020851	0.01133
		Si-Si	0.4564	.17376	.006570	0.00373
Lasaga <sup>2†</sup>	1.	O-O	146470.	.0	.03354	0.
		Si-O	165590.	.0	.032356	0.
Soules <sup>5</sup>	1.	O-O	16.90	.284	.029	0.
		Si-O	42.25	.275	.029	0.
		Si-Si	67.60	.266	.029	0.
		Na-O	29.58	.259	.029	0.
Kawamura <sup>6</sup>	1.	O-O	1.181	.3258	.0170	0.
		Si-O	1.146	.2641	.0165	0.
		Si-Si	1.112	.2024	.0160	0.
		Na-O	1.146	.2889	.0160	0.

† Expressed in the form of  $\phi_{ij}(r) = \frac{Z_i Z_j e^2}{4\pi\epsilon_0 r} + A_{ij} \exp(-\frac{r}{\rho_{ij}})$ .

in the potential.

The Stringer-Weber type<sup>9</sup> given by the following equation is widely used for a three-body potential form.

$$\Phi_{jik}^{SW}(r_{ij}, r_{ik}, \theta_{jik}) = \begin{cases} B_i (\cos\theta_{jik} - \cos\theta_{i^c})^2 \exp\left(\frac{\alpha_i}{r_{ij} - r_{i^c}} + \frac{\alpha_i}{r_{ik} - r_{i^c}}\right), & \text{for } r_{ij} < r_{i^c} \text{ and } r_{ik} < r_{i^c} \\ 0, & \text{for } r_{ij} \geq r_{i^c} \text{ or } r_{ik} \geq r_{i^c} \end{cases} \quad (3)$$

where  $r_{ij}$  and  $\theta_{jik}$  are the distance for  $i$ - $j$  atoms and the angle of  $j$ - $i$ - $k$  atoms, respectively, and  $B_i$ ,  $\theta_{i^c}$ ,  $\alpha_i$  and  $r_{i^c}$  are the potential parameters. Only two combinations of O-Si-O and Si-O-Si are considered for the three-body  $j$ - $i$ - $k$  potentials of silicates. To reproduce an ideal  $\text{SiO}_4$  tetrahedron, the value of  $\theta_{i^c}$  is chosen to be  $109.47^\circ$ . The parameter  $r_{i^c}$  corresponds to a cut-off distance for three-body terms, and is taken to be about 0.3nm for silicates.

There have been, however, very few studies including the three-body potentials mainly arising from the following two reasons.

- a. So called the "double loop" in the MD program must be altered to triple loop, and this leads to the increase of the computing time in proportional to  $N^3$ , where  $N$  is the number of atoms in the basic cell.
- b. The large memory arrays stored for the numerical values of the potential are required, or the potential values must be calculated within the triple loop if such an arrays are not used.

The three-body potential for silica have been employed firstly in the Monte-Carlo simulation.<sup>10</sup> Feuston and Garofalini,<sup>11</sup> and Vashishta *et al.*<sup>12</sup> proposed the three-body potentials for MD simulation of silica. Newell *et al.*<sup>13</sup> simulated the  $\text{Na}_2\text{O-SiO}_2$  system by using three-body potentials for O-Si-O and Si-O-Si combinations. The three-body potential parameters are listed in Table 2 for convenience.

**Table 2 Stringer-Weber Parameters for Silica and Silicates Proposed by Several Authors**

authors	$j$ - $i$ - $k$	$B_i/10^{-18}\text{J}$	$\theta_{i^c}/\text{deg.}$	$\alpha_i/\text{nm}$	$r_{i^c}/\text{nm}$
Feuston <sup>11</sup>	O-Si-O	18.0	109.47	.26	.30
	Si-O-Si	0.3	109.47	.20	.26
Newell <sup>13</sup>	O-Si-O	24.0	109.47	.26	.30
	Si-O-Si	1.00	109.47	.20	.26
Vashishta <sup>12</sup>	O-Si-O	0.807	109.47	.10	.260
	Si-O-Si	3.228	141.00	.10	.260

Obviously, non-empirical potential is preferable to the empirical one. However, it is difficult to give the definite comment about the actual validity of the three-body term at the present time. Nevertheless, the following results may be cited. Feuston and Garofalini<sup>11</sup> simulated the structures of vitreous silica with and without the three-body terms, and their results are shown in Fig. 4 for the radial distribution function (RDF) and the distributions of O-Si-O and Si-O-Si angles. It is found that the variation of the angles in the case of three-body potentials is smaller than that of pair potentials, and the essential structural features are insensitive to the selection of the potentials.

### III. Procedures of the MD Simulation on Silicates.

Although silicate melts are known to form rather complex network structure, the fundamental procedures of MD simulation is unchanged in comparison with those for simple liquids or molten salts. Of course, several cares must be paid in the simulation with relevant to the characteristic -Si-O- networks which provide their high viscosity and low ionic diffusivity. Differences from an ordinary simulation are as follows.

- a. To reproduce a realistic network structures, size of the basic cell and hence the number of atoms should be chosen sufficiently large.
- b. Since the Coulomb interactions are efficient in long distances, potential energy, forces and virials should be calculated by using the Ewald summation.
- c. In order to erase the memory of initial configuration, first hundreds or thousands steps must be carried out at high temperature, for

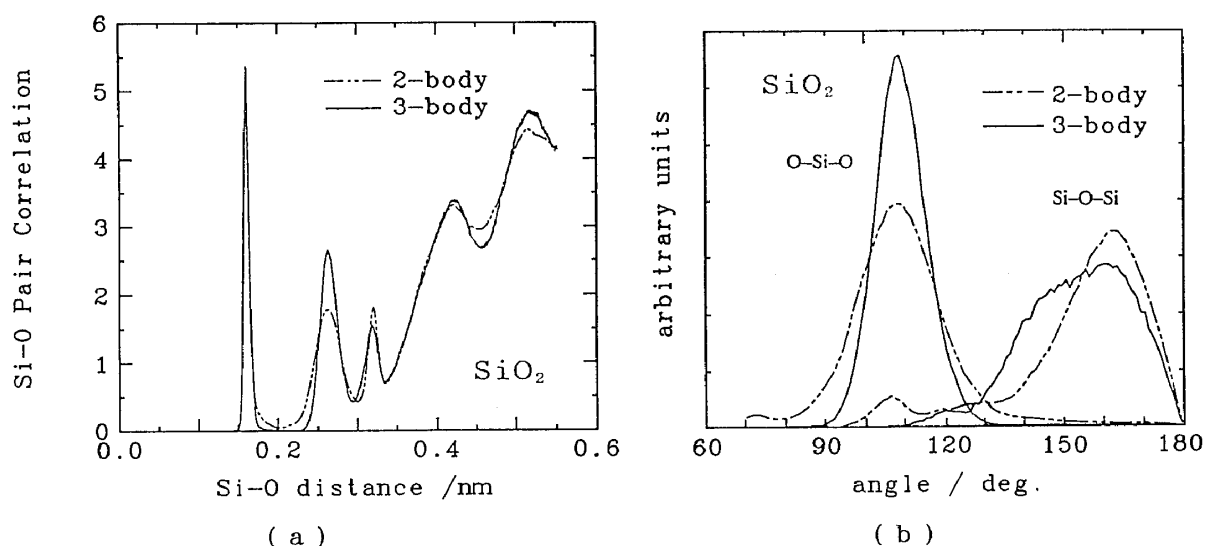


Fig. 4. Comparison of the results of MD simulation using two-body and three-body potentials: (a) radial distribution function, (b) the O-Si-O and Si-O-Si angle distribution (ref. 11).



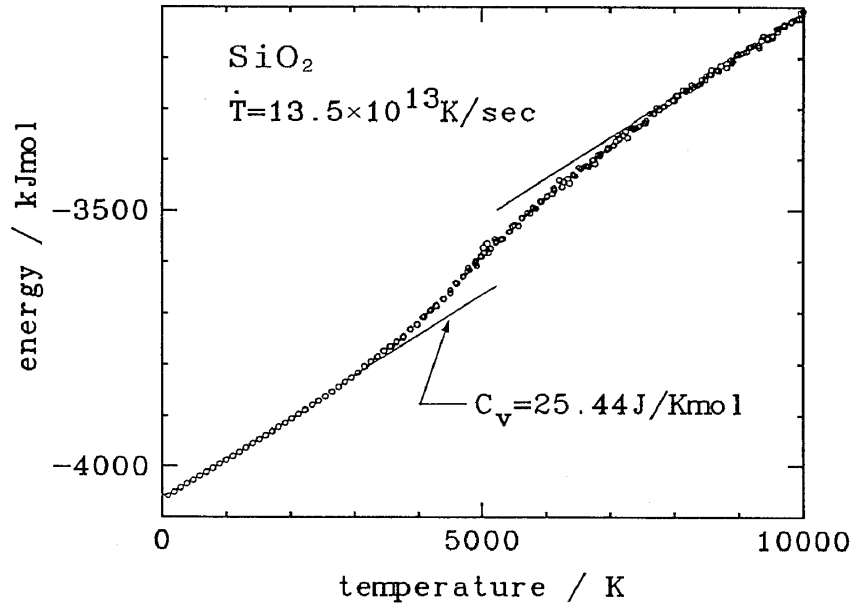


Fig. 5. Internal energy versus temperature of silica observed in MD simulation with a cooling rate of  $1.35 \times 10^{14}$  K/s (ref. 17).

example 6000K, where the ionic diffusivity is large. For precise discussions, if possible, several independent simulation should be carried out from different initial configurations.

- d. The quenching speed, equilibration time, and sampling time must be chosen properly by considering the long relaxation time.

#### IV. Some selected examples of the MD simulations for silicate melts

##### 1. Thermodynamic Properties

Various thermodynamic properties such as enthalpy, thermal expansivity, compressibility, and heat capacities of silicate melts can be estimated from the simulated values of temperature  $T$ , internal energy  $E$ , pressure  $P$ , and molar volume  $V$ .

The density is known to be a good criteria for judging the significance of interatomic potentials used in MD simulation by checking whether the density is correctly estimated or not. In the case of constant volume simulation employing the experimental density value, the resultant value of pressure must be compared with the assumed one.

The glass transition temperature,  $T_g$ , can be estimated in the simulation by the turning point in the curve of internal energy versus temperature. However, the simulated value of  $T_g$  is found to be several hundred degrees higher than the experimental one mainly due to the large cooling rate ( $\sim 10^{14}$  K/s) in the simulation. Kinetic mechanism of glass transition have also been investigated by MD simulation.<sup>14,15</sup> Habasaki<sup>16</sup> simulated the molten  $\text{Li}_2\text{O} \cdot \text{SiO}_2$  system at several

temperatures, and explained the glass transition mechanism by packing topology of oxygen ions around Li that the glass transition occurs when the cage structure of oxygen loses its freedom.

Soules<sup>17</sup> simulated the internal energy of molten silica up to 10,000K (Fig. 5) and found the specific heats at temperatures higher than 8000K are almost the same with the value in the glassy state.

## 2. Static Structures

*Short range structures* : Most of the MD studies for disordered system discuss the short range structures by using the RDF, pair correlation function (PCF), and the running coordination number (RCN). Comparison between calculation and experimental data is usually made with respect to the interference function or RDF determined by X-ray or neutron diffraction.<sup>1,11,18,19</sup> There have been found fairly good agreements between the simulation and the experimented data of silica glass as shown in Fig. 6.<sup>11,20</sup>

Angell *et al.*<sup>21</sup> simulated the structures of molten  $\text{Na}_2\text{O}\cdot 3\text{SiO}_2$  at high pressures, and reported the coordination number of oxygen around silicon increases from 4 to 6 with increasing pressure from 1 to 83MPa as shown in Fig. 7. It may be added in these results that the first and second neighbouring distances are hardly changed.

Iwamoto *et al.*<sup>22</sup> counted the number of bridging (BO) and non-bridging (NBO) oxygens for silicon in the  $2\text{Li}_2\text{O}\cdot \text{SiO}_2$  melt and glass. The simulated histogram of  $Q^n$  (where  $Q^n$  means the silicon ion of which number of coordinated BO's is  $n$ ) is consistent with that observed by Raman scattering.

Distribution of bonding angles for O-Si-O and Si-O-Si is another information

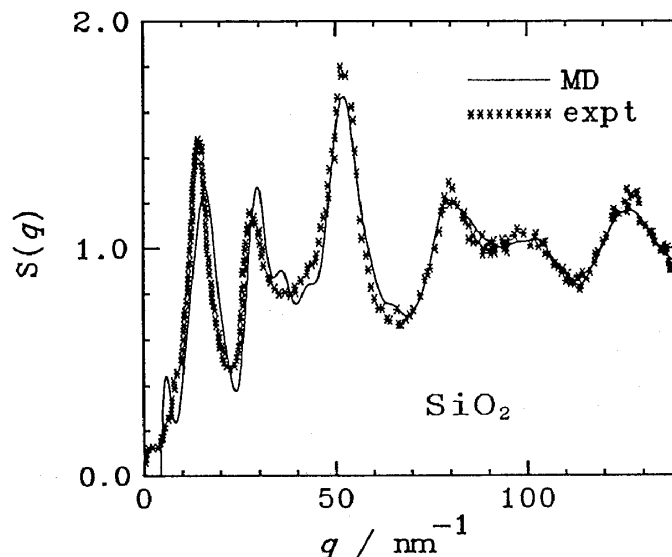


**Fig. 6.** Structure factor of  $\text{SiO}_2$  glass estimated by the MD simulation (ref. 11) together with the experimental data (ref. 21).

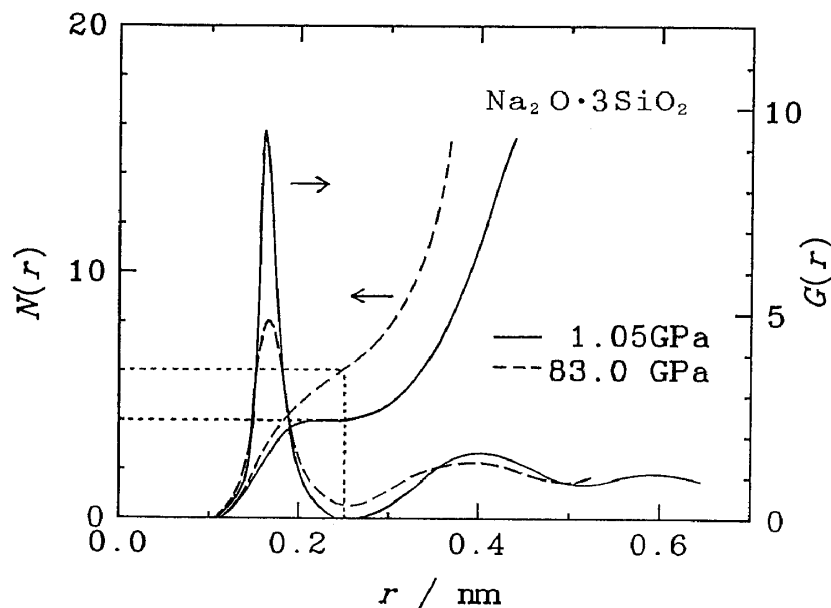


Fig. 7. The pair correlation function of Si-O and running coordination number of oxygen for silicon in the  $\text{Na}_2\text{O}\cdot 3\text{SiO}_2$  melt at low (a) and high (b) pressures (ref. 26).

of the local structures of silicates. The variation of O-Si-O angle from the mean value is a measure of the deformation of  $\text{SiO}_4$  tetrahedron, and the Si-O-Si angle itself is directly connected with the local network structures of silicates. It should be, however, kept in mind that they are sensitive to the potential employed as shown in Fig. 4(b).

Analysis of Voronoi polyhedra is also one way to obtain the information of the short range structures of disordered systems. However, Voronoi polyhedra analysis is not reported for silicates probably due to the fact that no unique definition of Voronoi polyhedra is given in multi-component system.

*Long range structures* : The description of 3-dimensional structures of -Si-O- networks is a key for the study on the structure of silicate melts. The RDF, RCN and RCN are not sufficient for describing the long range structures of silicates less sensitive to the structures at long distances. The variation of the bond in the nanometer order because they give only one-dimensional information and are angle or  $Q$  distribution provides the basic feature of the networks, but is not a good index for the long range structures.

Statistical analysis of  $-(\text{Si-O})_n$  rings or chains gives an almost unique index for explaining the long range structures of silicates. Matsui and Kawamura<sup>23</sup> reported by MD simulation that the 5 to 8 membered rings are frequently observed in the  $\text{CaAl}_2\text{Si}_2\text{O}_8$  melt. Ogawa *et al.*<sup>24</sup> counted the number of  $-(\text{Si-O})_n$  chains in molten  $\text{Na}_2\text{O-SiO}_2$  system, and suggested that the vibrational motion of these chains is one of the mechanisms of ionic diffusion in alkali-rich compositions.

**Fig. 8.** Anion diffusivities for several network-forming liquids as a function of  $1/T$  (ref. 33).

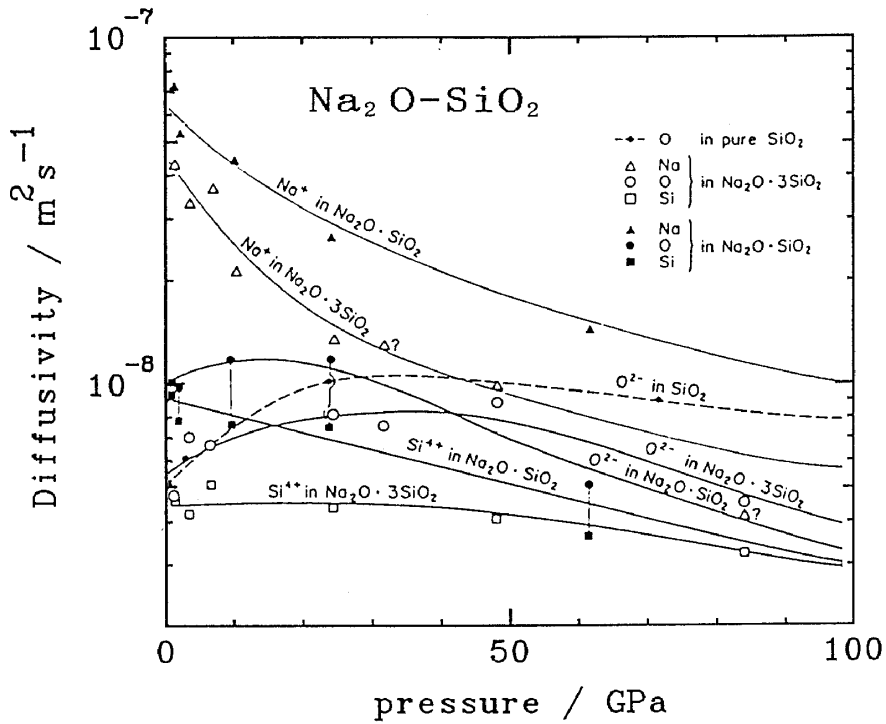
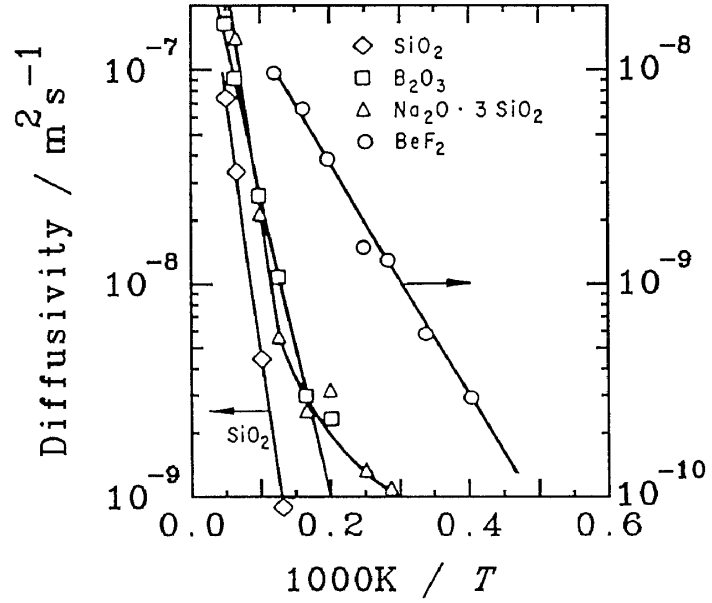


**Fig. 9.** Ionic diffusivities in  $\text{Na}_2\text{O}\cdot\text{SiO}_2$  melt at 6000K as a function of pressure (ref. 34).

*Surface structures* : The ordinary method for generating the free surface in the basic cell is used for silicates by filling the atoms in a part of the elongated (usually toward the  $z$  axis) column-like cell with the periodic boundary conditions.

Simulation of silicate surfaces have been investigated by several authors for

glassy states. Surface structures and their temperature dependences were investigated for silica and alkali-silicate glasses.<sup>25-28</sup> Behaviours of adhesive atoms on silica surface were also studied for Pt, Li, K, H<sub>2</sub>O, and Lennard-Jones atoms.<sup>29-32</sup>

### 3. Dynamic Properties

One of the advantages of MD technique is the direct sampling of atomic motions of interest. Such information cannot be obtained by other molecular simulation techniques such as Monte-Carlo and Molecular Mechanics.

*Self-diffusion coefficient* : The self-diffusion coefficient of  $i$  species,  $D_i$ , is calculated from velocities  $\mathbf{v}$  and positions  $\mathbf{r}$  as,

$$D_i = \frac{1}{3} \int_0^{\infty} \langle \mathbf{v}_i(t_0+t) \cdot \mathbf{v}_i(t_0) \rangle dt, \quad (4a)$$

or equivalently,

$$D_i = \frac{1}{6} \frac{d}{dt} \langle (\mathbf{r}_i(t_0+t) - \mathbf{r}_i(t_0))^2 \rangle. \quad (4b)$$

To obtain a quantitatively accurate result, simulation must be carried out for a sufficiently long time interval (100ps, for example).

Soules<sup>33</sup> has estimated the self diffusion coefficients of anions in several network-forming liquids as shown in Fig. 8. The anion diffusivity in pure SiO<sub>2</sub> is found to be very small compared with those in other oxide melts or molten salts. When Na<sub>2</sub>O is added to SiO<sub>2</sub>, on the other hand, the anion diffusivity increases and its temperature dependence shows deviation from the Arrhenius law. It may be worth mentioning that diffusivities of network-modifying ions such as Na, Li or K in alkali-silicates are about 1~2 orders faster than those of Si and O.

Angell *et al.*<sup>21,34</sup> estimated the diffusivities in the molten Na<sub>2</sub>O-SiO<sub>2</sub> system at high pressures and the results are given in Fig. 9. As shown in this figure, the values of  $D_{Si}$  and  $D_O$  depend irregularly on the pressure and they increase with increasing of pressure at lower pressures regions of 0 ~ 20GPa. This is consistent with the experimental result of shear viscosity at high pressures.<sup>35</sup> The diffusivity of Na<sup>+</sup> ions, on the other hand, show monotonic decrease as the pressure increases. These facts imply that the viscosity of silicate melts is dominated mainly by the mobility of the network forming ions.

The atomic motions relevant to the ionic diffusion in silica has been investigated by Woodcock *et al.*<sup>1</sup> Recently Kubiki and Lasaga<sup>36</sup> investigated the ionic motions in silica by using non-empirical potentials. The results are shown in Fig. 10. They suggested that the disconnection of #1 oxygen and connection of #5 oxygen occur through the temporal 5-fold state of central silicon just after

the large displacement of #1 oxygen.

*Shear viscosity* : Shear viscosity  $\eta$  may be calculated in MD simulation by the similar formulae to those for self-diffusion coefficient, as

$$\eta = \frac{V}{k_B T} \int_0^{\infty} \langle P^{\alpha\beta}(t_0+t) \cdot P^{\alpha\beta}(t_0) \rangle dt, \quad (5a)$$

where  $P^{\alpha\beta}$  is the off-diagonal element of stress tensor,  $k_B$  is the Boltzmann constant, and  $\alpha\beta$  corresponds to the permutation of  $xy$ ,  $yz$  and  $zx$ . The equivalent formula to eq.(5a) is given by

$$\eta = \frac{V}{2k_B T} \frac{d}{dt} \langle (G^{\alpha\beta}(t_0+t) - G^{\alpha\beta}(t_0))^2 \rangle, \quad (5b)$$

where  $\dot{G}^{\alpha\beta}(t) = P^{\alpha\beta}(t)$ . Ogawa *et al.*<sup>37</sup> calculated the shear viscosity of molten  $\text{Na}_2\text{O} \cdot 2\text{SiO}_2$  along the way similar to eq.(5a) and using other two independent methods. Based on these results, the MD simulation enables us to give semi-quantitative discussion only due to the present limitation of scales of few hundred atoms and few hundred picoseconds. The decay of stress autocorrelation functions of molten  $\text{Na}_2\text{O} \cdot 2\text{SiO}_2$  is given in Fig. 11.

*Other transport properties and structural relaxation* : Thermal conductivity and electrical conductivity of disordered systems can also be estimated, in principle, by the way similar to eqs.(4a) and (4b). However, no report is

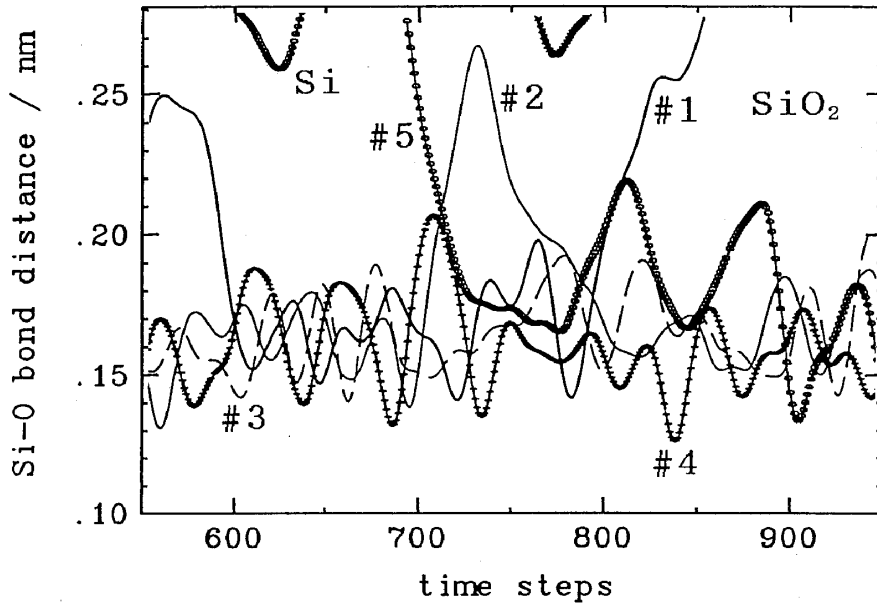


**Fig. 10.** Motions of nearest neighbour oxygens around a silicon in  $\text{SiO}_2$  melt at 6000K, 6MPa (ref. 36).

available for these transport properties of silicates at the present time.

Since the relaxation time in silicate melts is quite long, the structures obtained by the MD simulation gradually change even after getting the initial equilibration. Figure 12 shows the time variation of the local structures of silica during 75ps for the equilibrium simulation by Soules.<sup>17</sup> In this case, the structural relaxation takes place so as to decrease the defects of odd-number coordinated states with the time scale of 100ps.

### V. Concluding Remarks

Current views on the MD studies of silicate melts were surveyed by summarizing the results for their various properties, in order to facilitate the understanding of the present status including future prospects in this relatively new field. The techniques of MD simulation have not yet been completed. Of course, a number of preparations will be required before the full potentials of MD simulation can be assessed as a reliable tool for materials design.

- a. To improve the quantitative accuracy of the simulated results of silicate melts, more precise and realistic interatomic potentials must be given not only for Si-O, O-O and Si-Si pairs but also other possible pairs contained in silicate systems.
- b. Unknown factors arising from the initial configuration, cell size, or time schedule of the simulation must be determined with clear physical meaning.
- c. New index for describing the long-range network structures

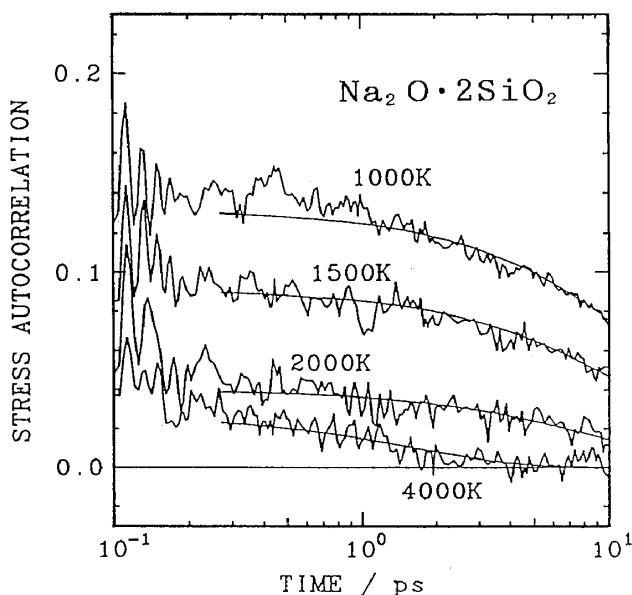
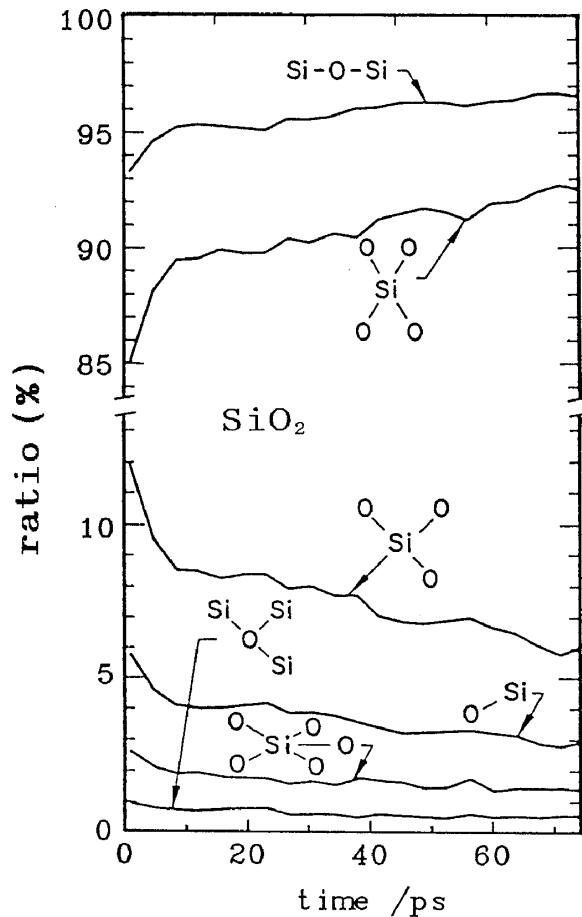


Fig. 11. Normalized stress autocorrelation function observed in MD simulation for molten Na<sub>2</sub>O·2SiO<sub>2</sub> (ref.37).



**Fig. 12.** Structural relaxation in SiO<sub>2</sub> melt observed in MD simulation at 1500K (ref. 17).

characterizing the structure of silicate melts is also strongly required.

Nevertheless, as mentioned in this paper with some selected examples, we have already built up a rather wider base for the useful MD method. When further studies with a highest priority could be continued for solving the above subjects, the MD method will be possible to provide a significant impact on the structure and various properties of silicate melts in a relatively short period.

*Acknowledgement* Authors are grateful to Drs. K. Kawamura and S. Kimura for their helpful advises.

#### References

1. Woodcock, L.V., Angell, C.A., and Cheeseman, P., *J. Chem. Phys.*, **65**, 1565 (1976).
2. Mitra, S.K., *Philos. Mag. B*, **45**, 529 (1982).
3. Soules, T.F., *J. Chem. Phys.*, **71**, 4570 (1979).
4. Kawamura, K., Science Dr. Thesis, University of Tokyo (1984).
5. Catlow, C.R.A., Freeman, C.M., Islam, M.S., Jackson, R.A., Leslie, M., and Tomlinson, S.M., *Philos. Mag. A, Phys. Condens. Matter Defects Mech. Prop.*,



- 58, 123 (1988).
6. Newton, M.D., O'Keefe, M., and Gibbs, G.V., *Phys. Chem. Miner.*, **6**, 305 (1980).
  7. Lasaga, A.C., and Gibbs, G.V., *Phys. Chem. Miner.*, **14**, 107 (1987).
  8. Tsuneyuki, S., Tsukada, M., Aoki, H., and Matsui, Y., *Phys. Rev. Lett.*, **61**, 869 (1988).
  9. Stringer, F.H., and Weber, T.A., *Phys. Rev. B*, **31**, 5262 (1985).
  10. Chongmu Lee, *J. Phys. C*, **19**, 5555 (1986).
  11. Feuston, B.P., and Garofalini, S.H., *J. Chem. Phys.*, **89**, 5818 (1988).
  12. Vashishta, P. Rajiv K. Kalia, Rino, J.P., and Ebsjo, I., *Phys. Rev. B*, **41**, 12197 (1990).
  13. Newell, R.G., Feuston, B.P., and Garofalini, S.H., *J. Mater. Res.*, **4**, 434 (1989).
  14. Kristensen, W.D., *Proc. Intern. Conf. on Computer Simulation for Materials Applications*, 561, Nat. Bur. Standards, Washington, DC. (1976).
  15. Mountain, R.D., Thirumalai, D., *Int. J. Mod. Phys. C*, **1**, 77 (1990).
  16. Habasaki, J., *Mol. Phys.*, **70**, 513 (1990).
  17. Soules, T.F., *J. Non-Cryst. Solids*, **123**, 48 (1990).
  18. Matsui, Y., Kawamura, K., *Nature*, **285**, 648 (1980).
  19. Hirao, K., and Soga, N., *J. Non-Cryst. Solids*, **84**, 61 (1986).
  20. Misawa, M., Price, D.L., and Suzuki, K., *J. Non-Cryst. Solids*, **37**, 85 (1980).
  21. Angell, C.A., Cheeseman, P., and Tamaddon, S., *Bull. Mineral.*, **106**, 87 (1983).
  22. Iwamoto, N., Umesaki, N., Takahashi, M., Tatsumisago, M., Minami, T., and Matsui, Y., *J. Non-Cryst. Solids*, **95-96**, 233 (1987).
  23. Kawamura, K., and Matsui, Y., *Materials Science of the Earth's Interior* (I. Sunagawa ed.), Terra-Reidel, Tokyo, Dordrecht, 3 (1982).
  24. Ogawa, H., Shiraishi, Y., and Kawamura, K., in preparation.
  25. Garofalini, S.H., *J. Chem. Phys.*, **78**, 2069 (1983).
  26. Levine, S.M., and Garofalini, S.H., *Surf. Sci.*, **163**, 59 (1985).
  27. Garofalini, S.H., and Zirl, D.M., *J. Vac. Sci. Technol. A*, **6**, 975 (1988).
  28. Rossky, P.J., and Lee, S.H., *Chem. Scr.*, **29A**, 93 (1989).
  29. MacElroy, J.M.D., and Raghavan, K., *J. Chem. Phys.*, **93**, 2068 (1990).
  30. Garofalini, S.H., *J. Am. Ceram Soc.*, **67**, 133 (1984).
  31. Garofalini, S.H., and Levine, S.M., *J. Am. Ceram Soc.*, **68**, 376 (1985).
  32. Garofalini, S.H., *Phys. Chem. Gla.*, **26**, 166 (1985).
  33. Soules, T.F., *J. Non-Cryst. Solids*, **49**, 29 (1982).
  34. Angell, C.A., Cheeseman, P., and Tamaddon, S., *Science*, **218**, 885 (1982).
  35. Kushiro, I., *J. Geophys. Res.*, **81**, 6347 (1976).
  36. Kubicki, J.D., and Lasaga, A.C., *Am. Mineral.*, **73**, 941 (1988).
  37. Ogawa, H., Shiraishi, Y., Kawamura, K., and Yokokawa, T., *J. Non-Cryst. Solids*, **119**, 151 (1990).